Power Conditioner for a PV Systems in The Alternating Current

LUIS DAVID PABON, EDISON ANDRES CAICEDO, JORGE LUIS DIAZ RODRIGUEZ, ALDO PARDO GARCIA.
Department of Electrical Engineering and Mechatronics
University of Pamplona
Ciudadela Universitaria, Km 1 via Bucaramanga, Pamplona
COLOMBIA
davidpabon@unipamplona.edu.co, aecaicedo@hotmail.com, jdiazcu@unipamplona.edu.co , apardo13@unipamplona.edu.co

Abstract- This paper presents a prototype of multilevel inverter that uses a modulation optimized in harmonic content of output voltages and that integrates a CD/CD converter, which allows regulating the value RMS of the output voltage of the inverter by controlling the voltage of the DC bus. In this way a control loop is made that allows to obtain optimum power quality in compliance with the IEEE 1159 (IEEE, 1995) and IEEE 519 standards (IEEE, 1992), avoiding phenomena such as sag, swell, Flicker, under voltage, etc. The prototype was implemented and the power quality is validated.

Key-Words: - Power conditioning, power quality, harmonics, power converter, multilevel converter, PWM, FPGA, optimization, genetic algorithm.

1. Introduction

In photovoltaic systems used to power loads in alternating current, it is essential to use inverters, since the solar panels generate energy in direct current and the use is in alternating component [1], [2].

Electrical Power Conversion from direct component to alternating component, try to find from direct current sources to obtain alternating current waveform to power AC (alternating current) machines from strategies called pulse width modulation (PWM) [3], these techniques lead to harmonic distortion problems and switching [4], [5].

To solve these problems and get a voltage waveform that is closer to a pure sine wave form, with the minimum switching of the power devices, a new family of inverters appears, called multilevel inverters [6] [7] [8].

Although the idea of using multiple voltage levels to perform the electrical conversion was proposed in 1975 by Baker and Lawrence in its US patent, the first multilevel inverter is implemented with the three step inverter introduced by Nabae, Takahashi and Akagi in 1981 [9]. Subsequently, several topologies of multilevel converters have been developed, which have in common the elementary concept of reaching stepped voltage waveform that are closer to a sine waveform [10] [11].

To bring the voltage waveforms of multilevel inverters to sinusoidal waveform, multiple works have been carried out to optimize the harmonic content [12], [13], [14]. These works try to eliminate the harmonics, either in selective orders [15] [16] [17] [18] or in a given range [19], however a definitive optimal value is not reached, so the subject is open for research.

Another problem of the CD/AC conversion in photovoltaic system, it is the variation of the voltage in terms of the load changes and fluctuations of the accumulator block or the variation of voltage in the solar panels from where the inverter is powered [15]. In inverters, the voltage regulation can cause the output voltages to overcome the established limits to conserve the power quality supplied to the load.

This work presents a prototype of multilevel inverter that by evolutionary techniques optimizes the harmonic content of the output voltages, integrates a CD/CD converter that allows regulating the root mean square (RMS) value of the inverter output voltage, by controlling the voltage of the DC bus. In this way, the power quality of the SFVs is optimized, avoiding phenomena such as sag, swell, flicker, undervoltage, overvoltage, interharmonics, frequency deviations and CD shifts and with a minimum of total harmonic distortion.

2. Multilevel Inverter of Two "Stages" Per Phase

To mitigate the power quality problems associated with the RMS value, the control of the tester is carried out on the direct current bus, through a CD/CD converter. The converter selected to perform this task, is the reducer converter not reduced elements inverter [19] [20] [21], which works with reduced elements the diagram of the CD/CD converter is shown in figure 1.

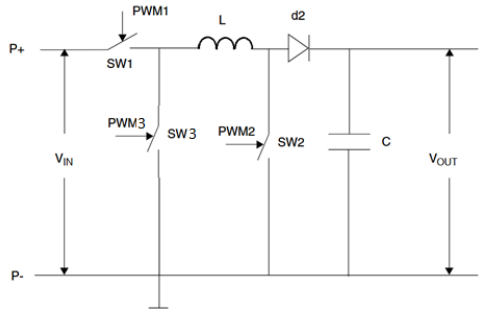

Figure 1. Circuit of the CD/CD converter.

In this work, the original topology is modified, by changing a blocking diode by the switching element SW3 in figure 1. This in order to perform a simpler activation process for switch SW1, using a simple bootstrap circuit.

To mitigate the phenomena associated with the waveform and generate voltages with harmonics optimization, the multilevel inverter topology selected is the three-phase cascade inverter type H asymmetric with common source by a 2-stage 1: 3 ratio, which generates line voltage with 17 steps, this topology is shown in figure 1 [16].

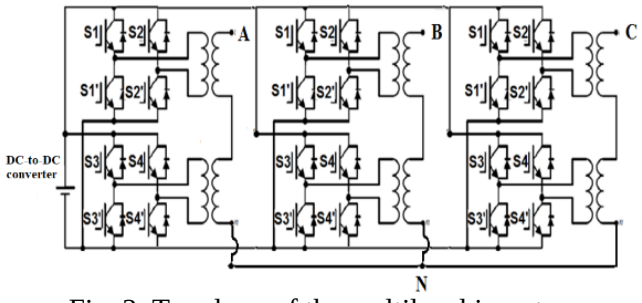

Fig. 2. Topology of the multilevel inverter.

These two inverters are connected in cascade to obtain the prototype of inversion and electrical power conditioning for PV systems that require an AC output.

3. Mathematical Modelling

Line voltage THD

The IEEE 519 of 1992 defines the total harmonic distortion as (3) [25]:

$$THD = \frac{\sqrt{\sum_{n=2}^{50} h_n^2}}{h_1} \cdot 100 \quad (1)$$

Where the harmonic h_1 is the fundamental component and h_n the peak of the harmonic n. Using this expression and previous works by the authors [13], [17], this expression becomes:

$$THD = \frac{\sqrt{\sum_{n=2}^{50}\left(\frac{1}{n}\left[\sum_{i=1}^{4}\sum_{j=1}^{Li}(-1)^{j-1}cos n\alpha_{ij}\right]\right)^2}}{\left[\sum_{i=1}^{4}\sum_{j=1}^{Li}(-1)^{j-1}\cos 1\alpha_{ij}\right]} * 100 \quad (2)$$

Where *n* takes odd values they do not multiple of three, that is to say 5, 7, 11, 13, 17, etc. and Li are the components of the vector L = [a b c d]. Which index how many angles each step has in the first quarter waveform of the modulation.

In the same way, the effective value can be defined in terms of harmonics such as:

$$Vline_{RMS} = \sqrt{\sum_{n=1}^{\alpha} Vrms_n{}^2} \quad (3)$$

Replacing an upper limit $h_{max} = 50$ the Vrms is determined by equation 2.26

$$Vline_{RMS} = \sqrt{\sum_{n=1}^{50} \frac{\left(\frac{4\sqrt{3}\,Vdc}{\pi n}\left[\sum_{i=1}^{4}\sum_{j=1}^{Li}(-1)^{j-1}cos n\alpha_{ij}\right]\right)^2}{2}}$$

$$for\ n = 5, 7, \ldots odd\ no \text{ multiple of three} \quad (4)$$

In this way, equation (2) defines the THD equation as the objective function, to be minimized by the optimization algorithm. Equation (4), second objective equation that will look for the desired effective value by the user, in this way the algorithm will look for a modulation with a certain RMS value defined as rated voltage by the user and with Total Harmonic Distortion as close to the zero percent.

In equations (2) and (4) the harmonics evaluated are the odd non-multiple of three, this is because the harmonics multiples of three cancel each other in the line voltages, being able to exist in the phases; however, since the inverter will be applied to a PV system where single-phase loads can be connected. The evaluation of two functions will contemplate the harmonics multiples of three in order to optimize the phase and line voltages.

4. Optimization Algorithm

Multiobjective genetic algorithms were used as an optimization technique, in order to make the THD equation as close as possible to zero and the V_{RMS}

equation to be as close as possible to 220 V, which will be the rated line voltage of the prototype, to achieve these objectives the authors propose the algorithm shown in figure 3.

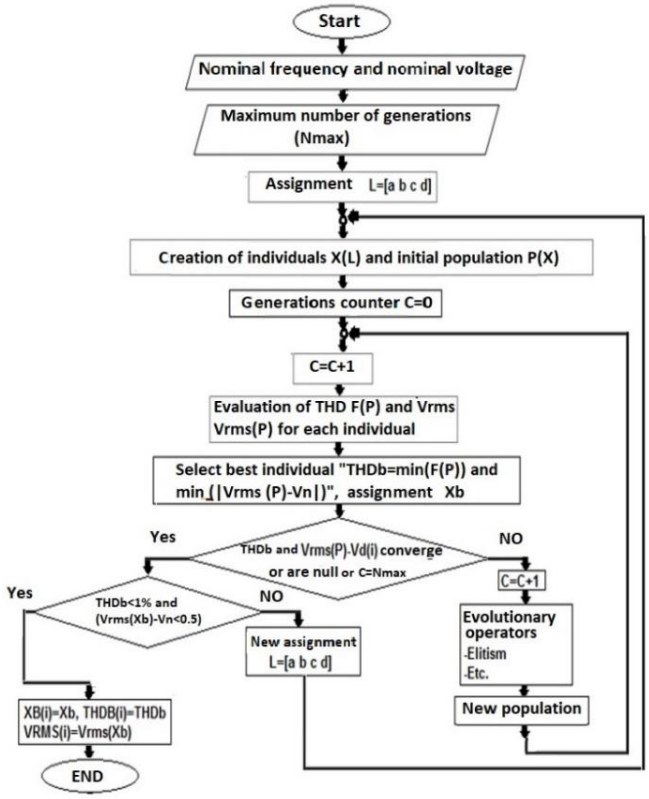

Figure.3 Multiobjective optimization genetic algorithm.

In the algorithm as the first the rated values are assigned, these are line voltage (Vn) and rated frequency (fn), then the maximum number of generations with which the multi genetic algorithm must operate is given by the user (Nmax). An initial vector L is assigned, to start the calculations of the RMS and THD value and the respective evolution.

The algorithm is responsible for assigning a vector of firing angles L = [a b c d], L contains the information of how many firing angles are to be generated in each of the four steps of the first quarter wave of the phase voltage of the converter. Then with this information, a population starts P(X) of 20 individuals X that are vectors of the form:

The algorithm with this data creates an initial population that evolves in terms of the performance of the two fitness functions given by the THD and VRMS equations. In each generation of evolution, the algorithm selects the individuals with lower THD and the RMS voltage value converges or if the THD is null and the RMS value is the desired or the maximum number of generations is met, or the evolutionary part of the algorithm ends. If these conditions are not given, the algorithm applies the evolutionary operators to the population and starts with another generation.

If this stage ends, the algorithm verifies that the THD is less than 0.1% and that the value of the RMS line voltage approaches the desired value with a margin of ± 0.5V, if this does not occur the algorithm assigns a new vector L = [a b c d] and iterate the evolutionary part again, until the conditions are achieved. When the conditions are met, the algorithm stores in a matrix the vector of trigger angles, its RMS voltage and its THD for the given frequency.

With the help of the Matlab® and the *gamultiobj* command, the algorithms corresponding to the mathematical model of the fitness functions (THD and VRMS equations) and their respective optimization by means of Multiobjective genetic algorithms were programmed. The population size for the algorithm is taken from 20 individuals, each individual (X) confirmed by the total of switching angles in the first quarter waveform of the phase voltage, accompanied by the vector L, which indicates to the program in charge of evaluating the fitness function the angles correspond to each step.

The rated value of the voltage was assigned to 220V, the rated frequency 60 Hz, and the direct current block of 45V.

5. Optimization Algorithm Results.

The vector L determined by the algorithm was L = [5 7 9 27], this means that the best individual is composed of 48 firing angles in the first quarter wave. The waveform of the phase voltage modulation of this individual is shown in Figure 4.

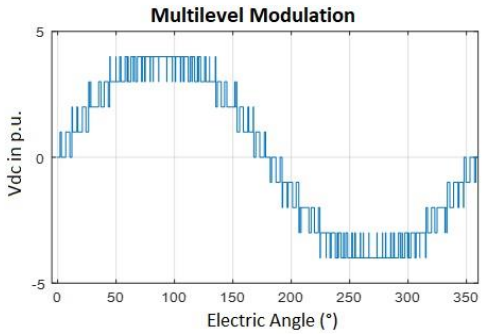

Figure 4. Waveform of the voltage modulation by phase.

This individual has an RMS value of 219.99 V, a THD of 0.00006% theoretical line, in phase the THD is 0.000067%, and the V_{RMS} value is 127. 011V, the

harmonic spectrum of this waveform with the voltage amplitude found by the genetic algorithm is shown in Figure 5.

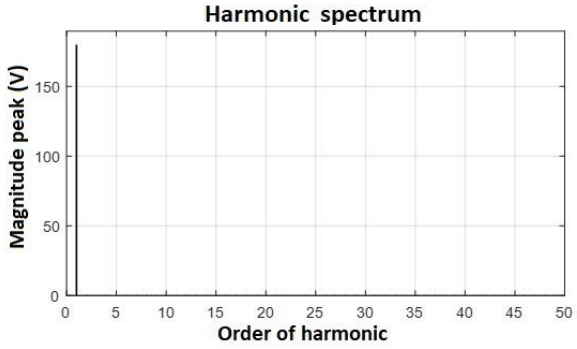

Figure 5 Harmonic spectrum of the phase modulation.

The spectrum of the phase voltage shows that there is no significant contribution of harmonics, presenting the harmonic content in the first 50 harmonics at first sight as null. The three-phase voltage system, generated by three phases that have the same waveform of Figure 4, but are shifted by electrical 120 °, is shown in Figure 6.

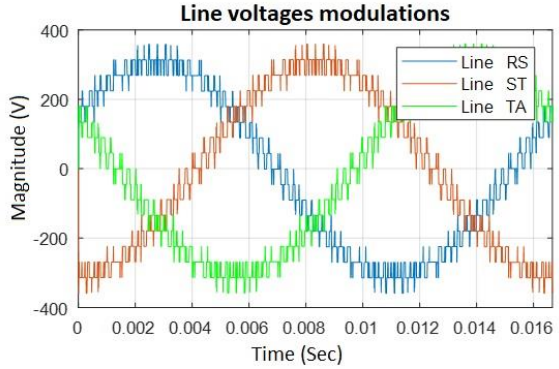

Figure.6 Line voltage modulations of the three-phase positive sequence system.

It is observed that in the line voltage appear additional steps and pulses, due to the subtraction that is made between the phases, the modulation by phase has 9 steps, while the line has 17 steps, the waveform is closer to the sinusoidal and the harmonic content decreases. The harmonic spectrum of the line voltages is shown in Figure 7.

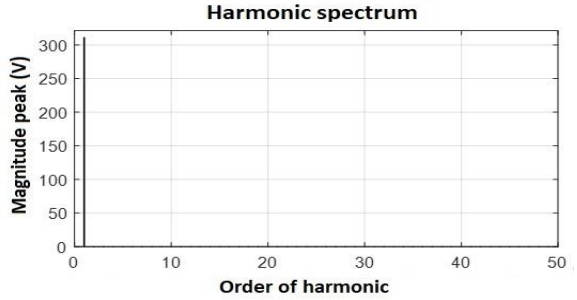

Figure 7. Harmonic spectrum of line voltage modulation

In this spectrum it is clear that the harmonic content is zero as of the phase voltages. The THD of this modulation is calculated at 0.0006% and the line V_{rms} value is 219.99V.

5.1 Implementation

The inverter and the CD/CD converter were implemented in a prototype of 2400 VA, with rated frequency of 60 Hz, the rated input voltage is 48 V, the maximum voltage at the input will be 70 V., and the rated voltage of the line voltages is 220V and the phase voltages of 127V. FPGA Virtex5 made the control of the CD/CD converter and the inverter, figure 8 shows the implementation of the electronics of the complete converter

Figure 8. System implementation.

5.2 Control Algorithm

For the voltage control that allows to maintain an optimum power quality, regardless of the loads variations in the accumulator block, the CD/CD converter was connected between the accumulator block and the multilevel inverter; this is the internal connection of the prototype. The CD/CD converter increases or decreases the input voltage of the inverter, in order to maintain the line voltage at the inverter output, regardless of the current required by the load or the voltage value given by the batteries. The measured variable is the line voltage of the inverter output; this voltage will be taken with the designed voltage sensor, which converts the RMS value of the voltage into a direct current value.

The output signal of the voltage sensor is acquired with the acquisition card NI USB 6009, which is connected to the PC with the control algorithm developed in Labview. This algorithm has its respective graphical interface where the set point of the voltage, which for the purpose of this research is 220V. The control commands from the Labview algorithm are communicated through

the serial port to the FPGA Virtex5, which controls the CD / CD converter by increasing or decreasing the output voltage, as required by the Labview control and controlling the multilevel inverter ensuring always the same waveform. That is, the control of the inverter is static, always giving the same signals so that the inverter always pulls out the same waveform.

In this way, the control loop is established. Figure 9 shows the block diagram of the different elements involved in the control of the prototype.

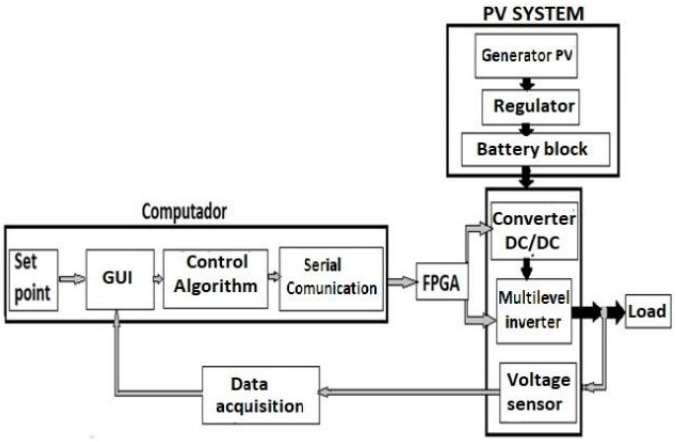

Figure 9. System implementation.

The set point of the system is assigned in 220V, this set point is assigned through a graphical interface made in Labview®, which allows to visualize the measured voltage and the desired voltage, as well as the control actions. The Labview algorithm has the scaling required for the sensor and the output variable, as well as the PID controller that is responsible for performing the control.

6. Experimental Results.

To verify the operation of the prototype, the inverter was powered by the accumulator block of the photovoltaic system through the CD/CD converter, a resistive three-phase load (variable rheostat) was connected in order to keep the test under control and be able to vary the operation points.

The assembly is shown in Figure 10 where the elements that make up the system are indicated.

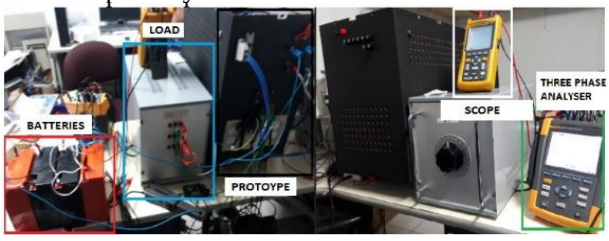

Figure 10. System assembly.

During the tests, the voltage and the currents that feed the load were measured and the power quality of the supply given by the inverter was evaluated. In the same way, the voltage of the accumulator block and the current circulating in the load were measured. The Fluke 434 network analyzer was used to evaluate the power quality of the inverter, which has the capacity to evaluate all the phenomena of power quality except transient phenomena. Likewise, the NI USB 6211 acquisition card used to capture the line voltage measurement from the sensor and signal from the Fluke DP 120 voltage sensor used to capture the accumulator block voltage was used.

In the test the load was varied and the accumulator block was discharged in a deep way, to observe the operation of the control loop and the power quality of the voltages and output currents, which are within the established by the standards as IEEE 1159 [26] and IEEE 519 [25] [27] [28].

The waveforms of the phase voltages captured by the power quality analyzer are shown in Figure 11.

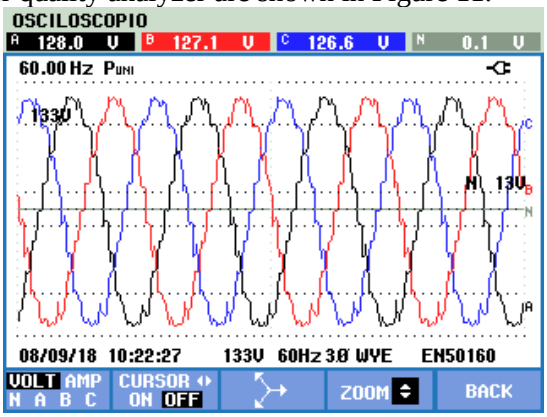

Figure 11. Phase voltages waveform.

It is observed in the figure that the three waveforms are identical, however, there are small differences in the RMS value due to the construction of the transformers; the percentage of unbalance of tensions is of 0.6%, which is below the 2% allowed in low tension. The spectrum of the phase voltages is shown in Figure 12.

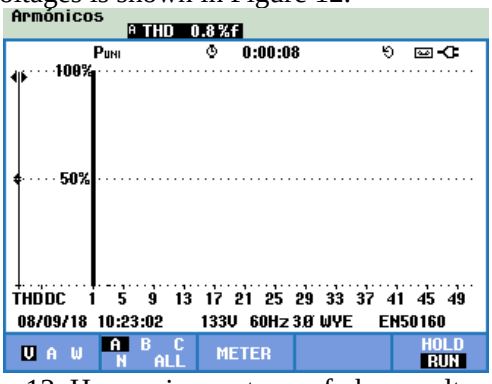

Figure 12. Harmonic spectrum of phase voltage V_A.

This spectrum shown in Figure 5 shows that there is no significant presence of harmonics of any order and the total harmonic content is 0.8%.

The waveforms of the line voltages are shown in Figure 13.

As can be seen in the figure, the three waves are identical in shape, presenting an almost sinusoidal waveform; however, they have different RMS values due to the differences presented by each of the phases due to magnetic coupling between phases and the construction of the transformers.

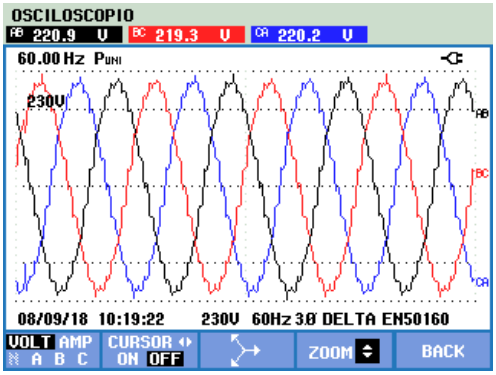

Figure 13. Line voltages waveform V_{AB}.

As can be seen in the figure, the three waves are identical in shape, presenting an almost sinusoidal waveform; however, they have different RMS values due to the differences presented by each of the phases due to magnetic coupling between phases and the construction of the transformers.

The harmonic spectrum captured by the analyzer for the line voltages is shown in Figure 14. This spectrum, which evaluates the first 50 harmonics, shows that there is no significant presence of harmonics of any order and that the total harmonic content is 0.5%, which is characteristic of a clean spectrum and which shows that the power quality, in terms of harmonic content, is optimal.

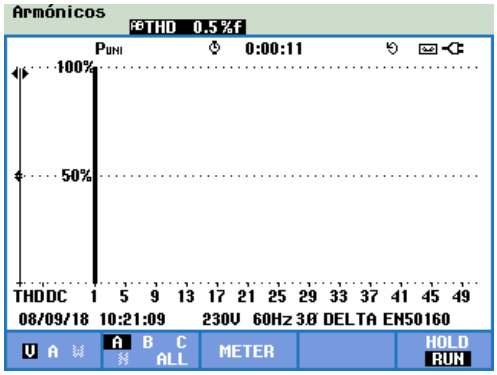

Figure 14. Harmonic spectrum of line VAB.

As for the output current of the converter, the waveforms are shown in Figure 15.

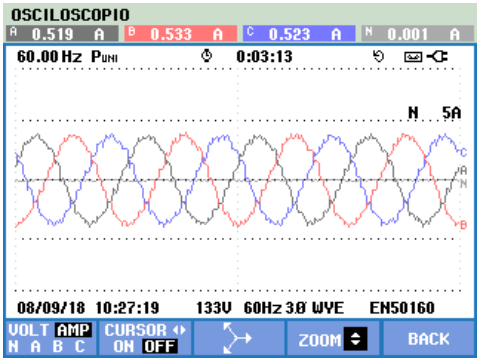

Figure 15. Electrical currents waveforms

Since the converter is connected in a star, the line currents are equal to the phase currents, as they are observed in an almost sinusoidal form, with small variations occurring. The three waveforms are identical in shape, presenting a nearly sine waveform. The harmonic spectrum is presented in figure 16.

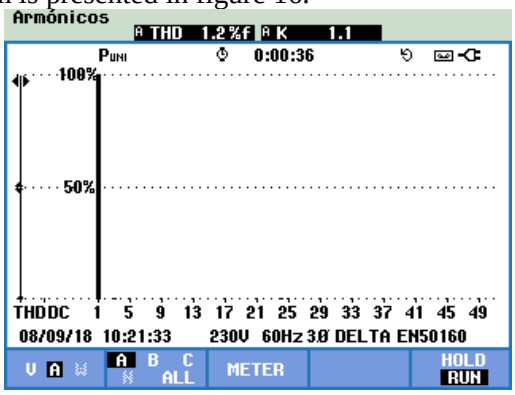

Figure 16. Harmonic spectrum of phase VA.

This spectrum shows that there is no significant presence of harmonics of any order and the total harmonic content is 1.2%, which is quite low.

Figure 17 shows the phasor diagram of the phase voltages and the line currents captured by the analyzer; the values associated with the voltages are shown. In this diagram, it is observed that the frequency is 60 Hz, and remains in this value independent of the load. Similarly, the values associated with the magnitudes of the voltages and phase angles of each of the phases are observed.

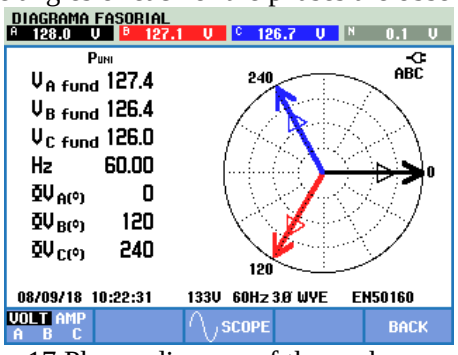

Figure 17 Phasor diagram of three-phase system.

The voltage system is perfectly balanced in phases, since the phase angle shows an exact "phase shift" of 120° between phases.

To show the behavior of the voltage at the output of the converter, Figure 18 shows the variation with respect to time, this figure is called the voltage profile

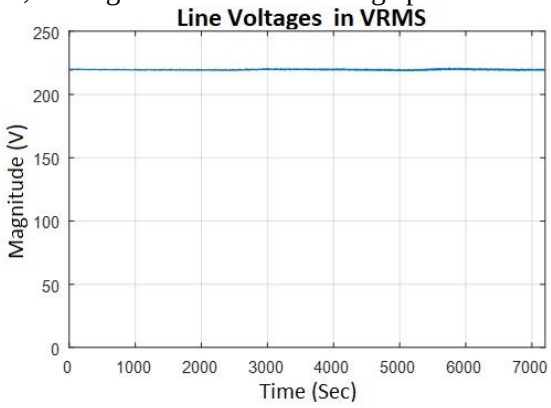

Figure 18. Inverter output line voltage profile

The RMS line voltage profile of the converter shows that the output behaves in a constant manner, presenting a small ripple that can be neglected because the voltage is always in the range of 90% and 110% of the rated voltage that is establishes as the normal operating range in energy quality. This means that, in the absence of voltage fluctuations, the energy quality phenomena associated with the RMS value are eliminated, these phenomena are sag, swell, overvoltage, undervoltage, interruptions and flicker. The ripple presented by the output voltage does not exceed the volt of magnitude, this ripple does not generate flicker since it is too low to be noticed by a lamp, and being always in the range of 90% to 10% of the rated voltage It can be said that it is free of energy quality phenomena.

The voltage profile of the accumulator block during the test is shown in figure 19. Here it is seen how the input voltage varies to the converter.

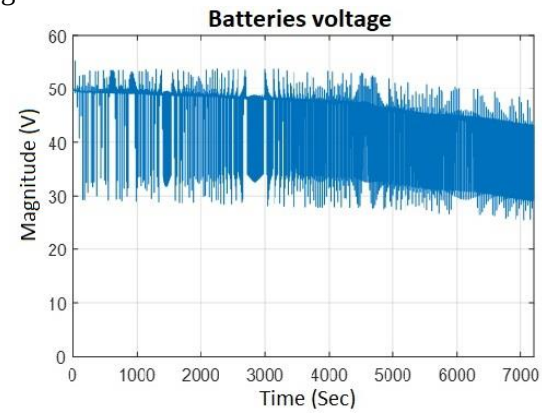

Figure 19. Voltage profile at the converter input.

The voltage profile of the accumulator block shows that there are strong variations in the input, due to the draft current required by the prototype. The average voltage decreases as time passes, the initial value of the accumulator block is 52 Volts, at the end of the test the accumulator block voltage is 43V. Despite the variations in the accumulator block and the voltage regulation that occurs over time, the voltage at the output of the converter remains constant over time. This means that the proposed control loop works in an adequate manner, managing to mitigate the possible swell, sag, undervoltage and overvoltage that may occur due to the voltage variation of the accumulator block. Figure 20 shows the report of the voltage profile of the AB line voltage recorded by the power quality analyzer.

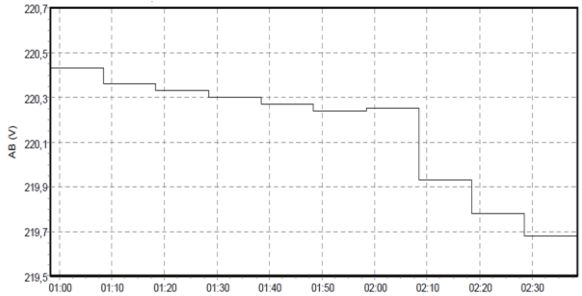

Figure 20.Voltage profile of the line V_{AB}

It was observed that the voltage variation at the start of the test until it ended was 0.7 volts; this variation is irrelevant if one takes into account that the accumulator block was discharged and that there were load variations during the test.

In figure 21, the record of the values of the first 25 harmonics and the THD for the AC line is shown. As you can see the maximum value of THDv registered, it is in the order of 0.6%; all harmonics are below or well below .04%, with records below 0.08% in most cases.

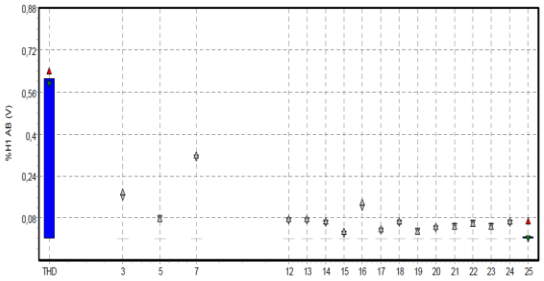

Figure 21. Harmonics registration for line $V_{AB.}$

Figure 22 shows the record for imbalances and frequency variations, the analyzer does not record any appreciable value of percentage of unbalance in the voltages or frequency variation, which validates that there are no events associated with this category.

Figure 22. Voltage unbalances and frequency variations.

As can be seen in the record of the tests carried out, the output of the converter has an optimum quality regardless of the load that is connected and the discharge that the accumulator block that feeds the prototype can suffer.

The power quality analyzer did not report events during the tests carried out independently that the load was changed or that the accumulator block was discharged and its voltage varied this confirms the operation of the prototype developed.

7. Conclusions

The prototype developed optimizes the power quality of photovoltaic systems by eliminating the possibility of phenomena such as sag, swell, undervoltage, overvoltage, harmonic distortion, flicker, frequency deviations, interharmonic distortion, subharmonic and CD component. The only phenomena that the team does not cover are transient phenomena and unbalances.

The harmonic contents found in the experimentation are very good both in the phase voltages and in the line voltages. In the same way the current also has optimized contents, however, they do not reach equal to the theoretically calculated ones, this is due to the presence of transformers that inject perturbations between phases and does not reproduce the pulses with accuracy. It is noteworthy that the harmonic contents found have very low magnitudes, reaching values of 0.6%.

In the validation, the power inverter was presented at different operation points demonstrated that the output power quality of the develop prototype was confortable.

ACKNOWLEDGEMENT

The authors gratefully thank to COLCIENCIAS and University of Pamplona development funds for supporting this project.

References:

[1] S. Deshpande and N. R. Bhasme, "A review of topologies of inverter for grid connected PV systems," in 2017 Innovations in Power and Advanced Computing Technologies (i-PACT), 2017, pp. 1–6.

[2] D. Barater, E. Lorenzani, C. Concari, G. Franceschini, and G. Buticchi, "Recent advances in single-phase transformerless photovoltaic inverters," IET Renew. Power Gener., vol. 10, no. 2, pp. 260–273, 2016.

[3] V. Gaikwad, S. Mutha, R. Mundhe, O. Sapar, and T. Chinchole, "Survey of PWM techniques for solar inverter," in 2016 International Conference on Global Trends in Signal Processing, Information Computing and Communication (ICGTSPICC), 2016, pp. 501–504.

[4] J Rodriguez, L Pabon, A P García THD improvement of a PWM cascade multilevel power inverters using genetic algorithms as optimization method, WSEAS Transactions on Power Systems, ISSN: 2224-350X. vol. 10, pp. 46-54, 2015.

[5] V Garrido, J L Diaz, A P Garcia. Analysis of the power quality using intelligent techniques. WSEAS Trans on Power Syst. ISSN: 2224-350X, v10, f 1, pp. 13–19, 2015.

[6] L Pabon, E A Caicedo, J L Diaz, A P Garcia. Configurable converter for performance assessment of cascaded multilevel power converters. WSEAS Transactions on Power Systems. ISSN: 2224-350X, v11, pp 199 – 209, 2016.

[7] S. A. Saleh and M. A. Rahman, "Modeling of Power Inverters," in An Introduction to Wavelet Modulated Inverters, IEEE, 2011, p. 1.

[8] S. A. Saleh and M. A. Rahman, "Introduction to Power Inverters," in An Introduction to Wavelet Modulated Inverters, IEEE, 2011, p. 1.

[9] A. Ruderman, "About Voltage Total Harmonic Distortion for Single- and Three-Phase Multilevel Inverters," IEEE Trans. Ind. Electron., vol. 62, no. 3, pp. 1548–1551, 2015.

[10] O Suarez, C Vega, E Sánchez, A González, O Rodríguez, A Pardo. Degradación anormal de p53 e inducción de apoptosis en la red p53-mdm2 usando la estrategia de control tipo pin. Revista Colombiana de Tecnologías de Avanzada. ISSN: 1692-7257, 2018.

[11] H. Abu-Rub, M. Malinowski, and K. Al-Haddad, "Multilevel Converter/Inverter Topologies and Applications," in Power Electronics for Renewable

Energy Systems, Transportation and Industrial Applications, IEEE, 2014.

[12] Larbi Djilali, Oscar J. Suarez, Aldo Pardo Garcia, Mohammed Belkheiri. First Sliding Mode Control of a DFIG-based Wind Turbine with mechanical part control. WSEAS TRANSACTIONS on SYSTEMS. E-ISSN: 2224-2678, 2018.

[13] B. Wu and M. Narimani, "Other Multilevel Voltage Source Inverters," in High-Power Converters and AC Drives, IEEE, 2017, p. 1.

[14]A. K. Koshti and M. N. Rao, "A brief review on multilevel inverter topologies," in 2017 International Conference on Data Management, Analytics and Innovation (ICDMAI), 2017, pp. 187–193.

[15] G. Ghosh, S. Sarkar, S. Mukherjee, T. Pal, and S. Sen, "A comparative study of different multilevel inverters," in 2017 1st International Conference on Electronics, Materials Engineering and Nano-Technology (IEMENTech), 2017, pp. 1–6.

[16] RÁ López, MG Angarita. AT Espinosa. Convertidores fotovoltaicos en módulos integrados basados en inversores de fuente-semi-cuasi–z: un nuevo esquema de control por modos deslisantes. Revista Colombiana de Tecnologías de Avanzada. ISSN: 1692-7257, 2014.

[17] HA Meza, JLM García, SS Mora. Estrategias de control mppt aplicadas en un convertidor dc/dc tipo boost para sistemas fotovoltaicos. Revista Colombiana de Tecnologías de Avanzada. ISSN: 1692-7257. 2018.

[18] V. Roberge, M. Tarbouchi, and F. Okou, "Strategies to Accelerate Harmonic Minimization in Multilevel Inverters Using a Parallel Genetic Algorithm on Graphical Processing Unit," IEEE Trans. Power Electron., vol. 29, no. 10, pp. 5087–5090, 2014.

[19] A Araque, JLD Rodríguez, AS Guerrero. Optimización por recocido simulado de un convertidor multinivel monofásico con modulación pwm sinusoidal de múltiple portadora. Revista Colombiana de Tecnologías de Avanzada. ISSN: 1692-7257, 2017.

[20] T. Jacob and L. P. Suresh, "A review paper on the elimination of harmonics in multilevel inverters using bioinspired algorithms," in 2016 International Conference on Circuit, Power and Computing Technologies (ICCPCT), 2016, pp. 1–8.

[21] M. Srndovic, A. Zhetessov, T. Alizadeh, Y. L. Familiant, G. Grandi, and A. Ruderman, "Simultaneous Selective Harmonic Elimination and THD Minimization for a Single-Phase Multilevel Inverter With Staircase Modulation," IEEE Trans. Ind. Appl., vol. 54, no. 2, pp. 1532–1541, 2018.

[22] A. Anurag, N. Deshmukh, A. Maguluri, and S. Anand, "Integrated DC–DC Converter Based Grid-Connected Transformerless Photovoltaic Inverter With Extended Input Voltage Range," IEEE Trans. Power Electron., vol. 33, no. 10, pp. 8322–8330, 2018.

[[23] J. L. D. Rodriguez, L. D. P. Fernandez, and A. P. Garcia, "Harmonic distortion optimization of multilevel PWM inverter using genetic algorithms," in 2014 IEEE 5th Colombian Workshop on Circuits and Systems (CWCAS), 2014, pp. 1–6.

[24] R. S. Weissbach and K. M. Torres, "A noninverting buck-boost converter with reduced components using a microcontroller," in Proceedings. IEEE SoutheastCon 2001 (Cat. No.01CH37208), 2001, pp. 79–84.

[25] "IEEE Recommended Practice and Requirements for Harmonic Control in Electric Power Systems," IEEE Std 519-2014 (Revision of IEEE Std 519-1992). pp. 1–29, 2014.

[26] "IEEE Recommended Practice for Monitoring Electric Power Quality," IEEE Std 1159-2009 (Revision of IEEE Std 1159-1995). pp. c1-81, 2009.

[27] L Pabon, J Diaz, A Pardo Garcia. Total harmonic distortion optimization of the line voltage in single source cascaded multilevel converter. WSEAS Transactions on System. ISSN: 2224-2678, v15, pp 110–120, 2016.

[28] L Pabon, E A Caicedo,J L Diaz, A P Garcia. A Genetic Optimized Cascade Multilevel Converter for Power Analysis. Communications in Computer and Information Science. ISSN: 1865-0929, v657, 2016.

[29] J Araque, J Díaz Rodríguez, A Pardo García. Optimization of the THD in a Multi-Level Single-Phase Converter using Genetic Algorithms, Recent Advances in Electrical Engineering Series, "Advances in Automatic Control, Modeling & Simulation", WSEAS press, ISSN 1790-5117, 2013.